Electrochemical Studies of Arsenite Oxidase: An Unusual Example of a Highly Cooperative Two-Electron Molybdenum Center†

Kevin R. Hoke,‡ Nathan Cobb,§ Fraser A. Armstrong,*,‡ and Russ Hille*,§

Inorganic Chemistry Laboratory, Oxford University, South Parks Road, Oxford OX1 3QR, England, and Department of Molecular and Cellular Biochemistry, The Ohio State University, Columbus, Ohio 43210-1218

Received September 23, 2003; Revised Manuscript Received December 8, 2003

ABSTRACT: Arsenite oxidase from *Alcaligenes faecalis*, an unusual molybdoenzyme that does not exhibit a Mo(V) EPR signal during oxidative−reductive titrations, has been investigated by protein film voltammetry. A film of the enzyme on a pyrolytic graphite edge electrode produces a sharp two-electron signal associated with reversible reduction of the oxidized Mo(VI) molybdenum center to Mo(IV). That reduction or oxidation of the active site occurs without accumulation of Mo(V) is consistent with the failure to observe a Mo(V) EPR signal for the enzyme under a variety of conditions and is indicative of an obligate two-electron center. The reduction potential for the molybdenum center, 292 mV (vs SHE) at pH 5.9 and 0 °C, exhibits a linear pH dependence for pH 5−10, consistent with a two-electron reduction strongly coupled to the uptake of two protons without a p*K* in this range. This suggests that the oxidized enzyme is best characterized as having an L_2MoO_2 rather than $L_2MoO(OH)$ center in the oxidized state and that arsenite oxidase uses a "spectator oxo" effect to facilitate the oxo transfer reaction. The onset of the catalytic wave observed in the presence of substrate correlates well with the Mo(VI/IV) potential, consistent with catalytic electron transport that is limited only by turnover at the active site. The one-electron peaks for the iron−sulfur centers are difficult to observe by protein film voltammetry, but spectrophotometric titrations have been carried out to measure their reduction potentials: at pH 6.0 and 20 °C, that of the [3Fe−4S] center is ∼260 mV and that of the Rieske center is ∼130 mV.

Molybdoenzymes are widely used in biology for oxygen atom transfer reactions, utilizing the Mo(IV) and Mo(VI) states to exchange oxygen atoms with substrates (*1*). Because these enzymes typically interact with one-electron redox partners, an intermediate Mo(V) state is usually observed, if only transiently, under a variety of conditions, e.g., in the course of oxidative−reductive titrations and freeze−quench kinetic experiments (*2*−*5*). The relative population of the paramagnetic Mo(V) intermediate, observable by EPR,[1] typically follows a "semiquinone-like" distribution with poised potential, analogous to that seen for flavin systems. This behavior is a reflection of the molybdenum center functioning in discrete Mo(VI)/Mo(V) and Mo(V)/Mo(IV) one-electron couples (*6*).

Arsenite oxidases catalyze the two-electron oxidation of arsenite to arsenate as the first step in a detoxification pathway that is important in the cycling of arsenic in the environment, as well as providing an alternate respiratory chain in certain organisms (*7*−*9*). The detoxifying enzyme from *Alcaligenes faecalis* has been examined crystallographically and is an $\alpha\beta$ dimer with a reduced molybdenum bis(molybdopterin) center ($L_2Mo{=}O$) and a [3Fe−4S] cluster in the larger subunit and a [2Fe−2S] Rieske cluster in the smaller subunit (*10*). The molybdenum center possesses two equivalents of the pterin cofactor; thus, arsenite oxidase falls in the dimethyl sulfoxide (DMSO) reductase family of enzymes (*1*). Arsenite oxidase is thus far unique, however, in that the protein does not provide a ligand to the molybdenum: the residue that is a serine, cysteine, selenocysteine, or aspartate in other members of this group is an alanine (Ala199) in arsenite oxidase. In this regard, the molybdenum center of arsenite oxidase more closely resembles the tungsten centers of enzymes such as the aldehyde: and formaldehyde:ferredoxin oxidoreductases and may represent a transitional structure from tungsten- to molybdenum-containing enzymes.

The oxidized enzyme exhibits an EPR signal due to the $[3Fe{-}4S]^{+}$ cluster ($S = 1/2$) while in the reduced state it displays a signal characteristic of the $[2Fe{-}2S]^{+}$ Rieske center (*11*). However, no EPR signal attributable to a Mo(V) state has been detected. This suggests that the Mo(V)

† This work was supported by the Human Frontiers in Science Program and the U.K. Engineering and Physical Sciences Research Council (F.A.A.) and the National Institutes of Health (GM 59953 to R.H.).

* To whom correspondence should be addressed. (F.A.A.) E-mail: fraser.armstrong@chem.ox.ac.uk. (R.H.) E-mail: hille.1@osu.edu.

‡ Oxford University.

§ The Ohio State University.

[1] Abbreviations: *A*, electrode area; CHES, 2-(N-cyclohexylamino)-ethanesulfonic acid; δ, peak width at half-height; *E*, electrode potential; EPR, electron paramagnetic resonance; *F*, Faraday constant; Γ, coverage of enzyme on the electrode (mol cm^{-2}); HEPES, N-(2-hydroxyethyl)-piperazine-N′-(2-ethanesulfonic acid); *i*, current; i_{lim}, limiting current at high driving force; k_{cat}, rate constant for catalytic turnover; k_0, rate of interfacial electron exchange at zero driving force; MES, 2-(N-morpholino)ethanesulfonic acid; K_M, Michaelis−Menten constant; n_s, stoichiometric number of electrons transferred in an electrode process; n_{app}, cooperativity coefficient for a two-electron process; PFV, protein film voltammetry; PGE, pyrolytic graphite edge; PIPES, piperazine-N,N′-bis(2-ethanesulfonic acid); PMS, phenazine methosulfate; *R*, gas constant; SHE, standard hydrogen electrode; SCE, standard calomel electrode; *T*, temperature; TAPS, N-tris(hydroxymethyl)methyl-3-aminopropanesulfonic acid; *v*, rate of enzyme turnover.

10.1021/bi0357154 CCC: $27.50
Published on Web 01/21/2004

oxidation state is inherently very unstable, resulting in a highly cooperative two-electron transition between the Mo(IV) and Mo(VI) oxidation states. Although it is frequently the case that the Mo(V) state is thermodynamically unstable in molybdenum-containing enzymes (*2*), it is unprecedented that the destabilization is so extreme that no accumulation of the Mo(V) state is detectable by EPR during a reductive titration.

To investigate the electrochemical properties of arsenite oxidase further, we have undertaken a study using protein film voltammetry (PFV), a technique that probes the oxidation−reduction transitions and catalytic activity of protein molecules adsorbed on an electrode (*12*). In doing so, we have been able to exploit the appearance of a nonturnover signal due to reversible electron exchange between the electrode and the active site in the absence of substrate; this signal consists of oxidation and reduction peaks having a narrow width and sharpness consistent with a high degree of cooperativity for the transfer of two electrons (*13*−*15*). The limiting situation for cooperative two-electron transfer occurs if the second electron transfers to a center with potential that is substantially more positive than that for the first, resulting in the complete destabilization of the intermediate state. Thus, while the one-electron potentials required to form the Mo(V) state are too high or too low for oxidation or reduction of the enzyme, respectively, a two-electron transition between Mo(IV) and Mo(VI) is readily accessible. The high degree of cooperativity reported here establishes that the molybdenum center of arsenite oxidase functions effectively as an obligate two-electron acceptor.

MATERIALS AND METHODS

Electrochemical Measurements. All buffers and reagents used were commercially available and of high purity (typically 99+%). The substrate, sodium *meta*-arsenite ($NaAsO_2$), was obtained from Fluka (≥99.0%). *CAUTION:* arsenic-containing materials should be handled carefully to limit exposure to the researcher and to prevent introduction into the environment. Arsenite oxidase was prepared and purified in the oxidized state and assayed as described previously (*11*) and stored in liquid nitrogen until required. Thawed aliquots were centrifuged and passed down a Sephadex G-25 gel filtration column prior to use. For voltammetry, the PGE working electrodes were constructed as described previously (*16*, *17*), screening the electrodes for clean background voltammetry before each usage. For nonturnover experiments, the geometric surface area was 0.12 cm^2 while for catalytic experiments with a rotating disk electrode in the presence of substrate, the geometric surface area was 0.03 cm^2. In either case, the electrode was prepared for enzyme adsorption by polishing with an aqueous slurry of 1.0 μm alumina (Buehler) followed by brief sonication in Millipore-Q purified water. This generates a clean, rough surface that has a variety of hydrophilic functionalities and is well-suited for protein adsorption. A small aliquot of arsenite oxidase solution was applied directly to this freshly activated electrode surface. Cyclic voltammetry was performed under an argon atmosphere using potentiostats and other equipment similar to that described elsewhere (*16*, *18*). Buffers consisted of 100 mM sodium chloride with 20 mM MES (pH 6) or a 20 mM mixture of MES/PIPES/TAPS/CHES (for a variety of pH values). To optimize enzyme binding to the electrode, most voltammetry was carried out at 0 °C in a water-jacketed working cell with a SCE kept at 20 °C in a long sidearm linked to the sample compartment by a Luggin capillary tip. Potentials were related to the SHE using the conversion SHE = SCE + 244 mV at 20 °C (*14*). Data refinements, such as deconvolution, Fourier filtering, and polynomial baseline subtraction (*18*), were carried out using in-house software running under MacOS X.

Spectroscopic Determination of Fe−S Potentials. Reduction potentials for the iron−sulfur centers of arsenite oxidase were determined using the method described by Massey (*19*), in which the enzyme is titrated reductively using xanthine oxidase and mediators. When xanthine oxidase is allowed to oxidize excess xanthine in the absence of oxygen, the electrons are passed on via mediators to the enzyme of interest. Competition between the various redox-active centers for the electrons is revealed by changes in optical absorbance. The ratios of oxidized and reduced states for each center are obtained from the fractional changes in absorbance at a wavelength that corresponds predominantly to a specific center. Comparison of these ratios at any point in the titration gives the reduction potential of one center (A) relative to another (B), as expected from the Nernstian relationship:

$$E_A^{\circ} + \frac{2.303RT}{n_A F}(\log [\text{ox/red}]_A) = E_B^{\circ} + \frac{2.303RT}{n_B F}(\log [\text{ox/red}]_B) \quad (1)$$

Spectrophotometric reductive titrations of arsenite oxidase were performed using a Hewlett-Packard 8452A photodiode array spectrophotometer and associated software. Xanthine oxidase from bovine milk was produced at The Ohio State University as described previously (*20*). Arsenite oxidase (20 μM) was mixed with xanthine oxidase (0.2 μM), oxidized with ferricenium hexafluorophosphate, and then passed down a Sephadex G-25 column to exchange with 20 mM MES buffer, pH 6.0, at 20 °C. The oxidized enzyme mixture, along with 2 μM benzyl viologen, was protected from light and extensively degassed with argon in an anaerobic cuvette before the reaction was initiated by addition of degassed xanthine solution to 250 μM. Some runs also contained 25 μM PMS as an internal reference, using freshly prepared stock solutions that were protected from air and light.

RESULTS

Noncatalytic Voltammetry. The cyclic voltammetry at pH 5.9 and 0 °C shows a small but clearly visible signal with oxidation and reduction peaks in the region of 300 mV (Figure 1). This signal does not appear in the absence of enzyme. The peaks lie upon the capacitative background current that is typical for the PGE electrode and which can be subtracted by a routine procedure (*18*). The background correction (Figure 1, center) reveals a sharp signal centered at 292 mV. This signal is the only distinctive feature in the cyclic voltammogram, and in no case could we confidently distinguish from the background current any isolated one-electron signals attributable to the iron−sulfur clusters of the enzyme.[2] Both oxidation and reduction peaks are narrow, with an average half-height width of 63 mV, significantly less than the theoretical value for a one-electron transfer, 83

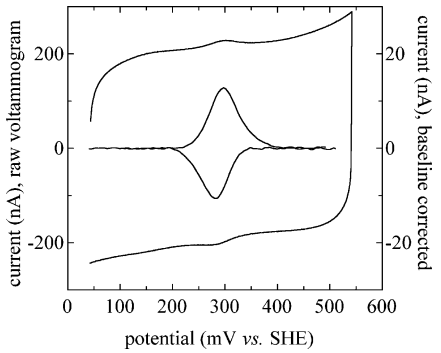

FIGURE 1: Voltammogram of arsenite oxidase adsorbed on a stationary PGE electrode, showing (inset) the signal after polynomial baseline correction. Conditions are as follows: pH 5.9; 20 mM MES; 100 mM NaCl; temperature, 0 °C; scan rate, 20 mV s^{-1}.

mV at 0 °C (*13*, *14*). This is significant since the width, δ, decreases as the apparent number of electrons transferred in a cooperative manner, n_{app}, increases ($n_{app} = 3.53RT/F\delta$). Thus, the coefficient n_{app} becomes a measure of the degree of cooperativity between the two one-electron transfers, although it is important to recognize that any environmental inhomogeneity within the adsorbed protein layer can decrease the apparent cooperativity (*13*).

To interpret the voltammogram, attempts were made to deconvolve the observed signal into multiple one-electron peaks with varying values of the "cooperativity coefficient", n_{app}. It was not possible to explain the signal in terms of the superposition of multiple one-electron signals, and the best fits for either scan direction required a two-electron peak with an n_{app} value of at least 1.4, and a potential quite close to the total peak maximum (Figure 2). From the peak areas for the best examples, the electroactive coverage was estimated at less than 2 pmol/cm^2, assuming two electrons for the couple(s) under the signal and a perfectly smooth electrode surface with an area of 0.12 cm^2; clearly with such a low coverage, it is difficult to rule out the presence of any broader one-electron components beneath the two-electron signal.

Increasing the pH shifts the signal to lower potential but also gives peaks that are slightly sharper, as shown in Figure 2. The average peak potential was measured over the pH range 5−10, and the resulting pH dependence is shown in Figure 3. The data fall on a straight line over the entire pH range with a slope of −59 mV/pH unit, similar to the value of −54 at 0 °C expected for a proton/electron ratio of 1.0. Therefore, assuming a two-electron process, as is consistent with the peak width, two protons are also transferred during oxidation and reduction of the enzyme, with no indication of any p*K* transitions due to ionizable groups in this pH range.

Reduction Potentials of the Fe−S Centers. It is known that during the course of reductive titrations of arsenite oxidase, the EPR signal for the [3Fe−4S] cluster begins to disappear before that of the Rieske center appears; therefore, the [3Fe−4S] center must have the higher potential (*11*).

[2] A variety of coadsorbates, such as polymyxin, heparin, and detergents, were tested for their ability to improve the low electroactive coverage, but the usual outcome was the removal of the signal altogether; similarly, electroactive coverage was difficult to maintain outside a pH of 5−9.

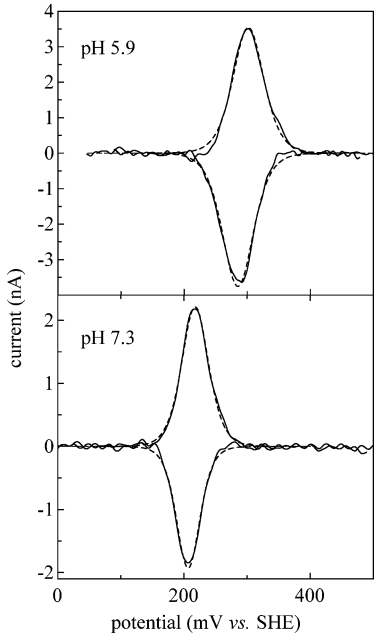

FIGURE 2: (Upper) Fitting the baseline-subtracted voltammogram at pH 5.9 requires modeling the peaks with $n_{app} = 1.4$ for both the oxidized and the reduced directions (solid lines represent the experimental data, and dashed lines represent the fit). (Lower) At pH 7.3, the peaks appear at lower potential and appear slightly sharper, with $n_{app} = 1.6$. Conditions are as follows: 20 mM MES (pH 5.9) or HEPES (pH 7.3); 100 mM NaCl; temperature, 0 °C; scan rate, 5 mV s^{-1}.

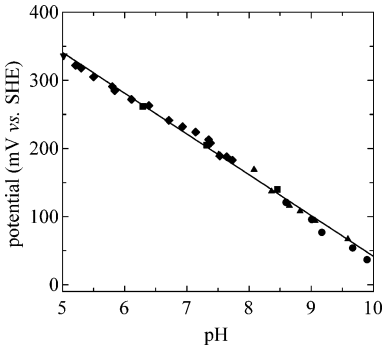

FIGURE 3: pH dependence of the reduction potential for the two-electron signal at 0 °C. The different symbols denote measurements from different films. The slope is −59 mV per pH unit, similar to that predicted for a 1:1 proton/electron ratio.

As the Fe−S clusters are not revealed distinctively by PFV, the potentials of these centers were determined using spectrophotometric reductive titrations. We employed the method described by Massey (*19*), using the xanthine: xanthine oxidase system as a source of electrons and PMS as a standard. Results are shown in Figure 4, where it is seen that the oxidized and reduced forms of PMS do not absorb strongly in the long wavelength region of the spectrum of arsenite oxidase.

The spectrum of oxidized PMS has two peaks at 388 and 368 nm that are bleached as the dye is reduced. Noting that the spectra of oxidized and reduced arsenite oxidase are nearly parallel in this region (as shown in Figure 4C), we were able to separate the contribution of the enzyme from that of PMS by using the fact that the difference in the absorbance of the enzyme at 380 and 370 nm is nearly constant during the reduction (as shown in Figure 4F), in a manner analogous to an isosbestic point. Therefore, monitor-

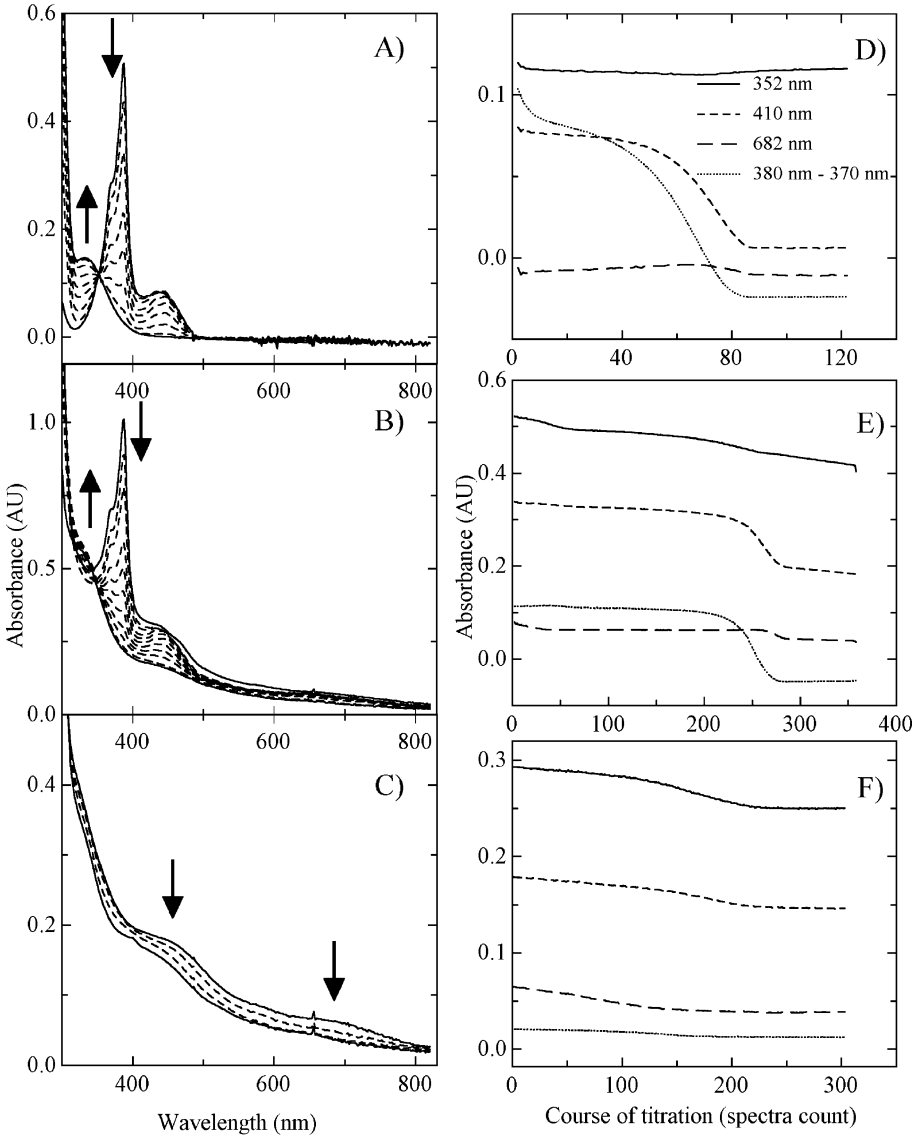

FIGURE 4: Spectral overlays showing reductive titrations for (A) PMS alone, (B) arsenite oxidase and PMS together, and (C) arsenite oxidase alone. Arrows denote the direction of the change in absorbance over time. From these, the extent of reduction is monitored at various wavelengths for (D) PMS alone, (E) arsenite oxidase and PMS together, and (F) arsenite oxidase alone.

ing the difference in 380 and 370 nm absorption over the course of the titration reveals the extent of reduction of the dye alone. In addition, 352 nm is an isosbestic point for the spectral change associated with the reduction of PMS, allowing the reduction of the enzyme alone to be monitored at this wavelength. There are two phases for the reduction of the enzyme in the course of the experiment—the first corresponds primarily to the reduction of the [3Fe−4S] and Mo sites and the second to that of the Rieske center. From the spectral change at 352 nm, it is thus possible to obtain the proportion of oxidized and reduced forms for each center independently.

It can be assumed that the enzyme is initially fully oxidized and that the first titration is complete (i.e., the higher potential site(s) fully reduced) when the absorbance at 352 nm begins to level out approximately midway through the entire titration (Figure 4E). Using the extent of change in absorbance as a measure of the fraction reduced for the site, when this initial phase of the titration is at its midpoint (i.e., 50:50 oxidized/reduced), the logarithm of the oxidized/reduced ratio (plotted on the *x*-axis) is 0 and the solution must be at the midpoint potential of the higher potential site, according to the Nernst relation given in eq 1. However, in this case, the solution is also at a potential where the logarithm of the ratio of the PMS oxidized/reduced ratio is 2.3 (the value of the higher *y*-intercept in Figure 5A); that is, the PMS is mostly oxidized and hence at that point in the titration the solution potential is well above 92 mV, the midpoint potential of the dye (*21*). Using eq 1 and the *y*- and *x*-intercepts from Figure 5A, we obtain a value of 210−230 mV vs SHE at 20 °C and pH 6. Considering that the accuracy of the spectrophotometric reductive titration decreases as the potential differs from the reduction potential of the standard, this is consistent with the value observed from PFV for the Mo site: 254 mV when measured at 20 °C and pH 6.0, where the conditions are matched to those of the titration. A similar approach applied to the later portion of the titration gives the reduction potential of the Rieske center (from the lower line in Figure 5A): approximately 33−44 mV higher than PMS, i.e., 130 mV vs SHE.

PMS is unstable to both air and light, which made it necessary to keep stock solutions anaerobic and covered.

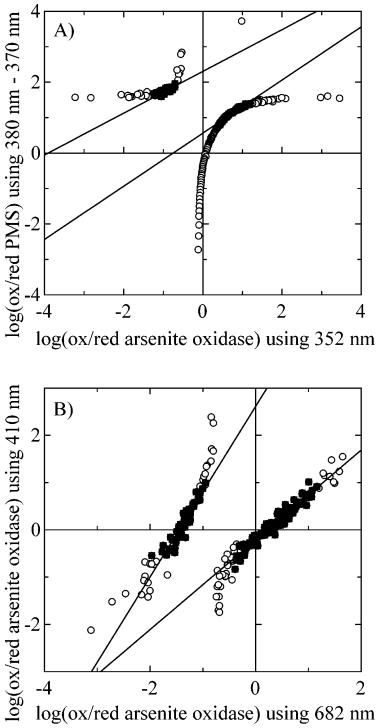

FIGURE 5: (A) Use of log−log plots to determine the arsenite oxidase reduction potentials relative to PMS. (B) The log−log plot to determine the reduction potentials of Fe−S centers relative to the Mo center in the absence of PMS. Solid symbols represent the subset of data taken as being the most linear and used to determine the *y*- and *x*-intercepts.

Despite such measures, it was generally considered unreliable to monitor wavelengths below 500 nm, apart from the 352 nm isosbestic point, as absorbance changes corresponding to PMS alone (Figure 4D) occur at similar wavelengths as for the Fe−S centers. Therefore, the reductive experiment was repeated in the absence of PMS to find the relationship between changes in the region of 410 nm (primarily due to the Fe−S centers) and those at 682 nm (dominated by the Mo center). Two distinct transitions in Fe−S absorption were observed (Figure 4F): one early on in the course of the titration (i.e., of higher reduction potential) and another somewhat later (of lower potential). The first, identified as the [3Fe−4S] center from the earlier EPR work, is approximately 10 mV higher in potential than the Mo center, or ∼260−270 mV vs SHE at pH 6 and 20 °C. The second transition, due to the Rieske center, is at least 40−150 mV lower in potential or about 110 mV vs SHE at the lower limit. This is consistent with the value determined in the presence of PMS, again considering the increased uncertainty as one extrapolates far from the reference potential.

Catalytic Voltammetry. The catalytic activity of arsenite oxidase was examined voltammetrically using a rotating disk electrode. When doing so, the electrode was rotated at sufficient frequency (2400 rpm) to ensure that the catalytic current is not controlled by the rate of transport of substrate to the electrode. The catalytic current results from the continual oxidation of the enzyme following reduction by substrate. It appears in the same region of potential as the Mo center and follows a similar pH dependence (Figure 6). No response with arsenite was seen in the absence of enzyme. As seen from the magnitude of the catalytic current, the

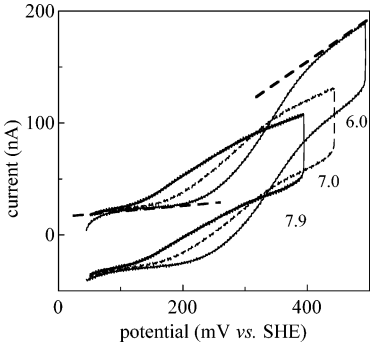

FIGURE 6: Catalytic voltammograms for a film of arsenite oxidase, showing the increase in activity obtained as the pH is lowered (data obtained at 0 °C in the order pH 7.9, 7.0, and 6.0 to minimize film loss). The voltammograms exhibit greater slope at the higher potential limit than at lower potential, as indicated on the pH 6.0 voltammogram by dashed lines. Conditions are as follows: 100 μM arsenite; 20 mM mixed buffer; 100 mM NaCl; electrode rotation rate, 2400 rpm; scan rate, 10 mV s^{-1}; temperature, 0 °C.

enzymatic activity increases as the pH is lowered to 6.0, as was also observed in standard solution assays (*11*).

To obtain kinetic parameters from a sigmoidal catalytic voltammogram, one typically uses the limiting current at high overpotential. However, the catalytic voltammetry for arsenite oxidase exhibits a more complex shape that is heavily influenced by substrate concentration and temperature. Figure 7 shows that as the catalytic current increases, either with increasing substrate concentration (A) or temperature (B), the wave converts from a sigmoidal form to one in which at high potential there is a marked residual slope from which a limiting plateau cannot be determined (this is also indicated with dashed lines in Figure 6). This residual slope has been attributed to contributions from those enzyme molecules that, presumably due to less favorable orientation(s) on the electrode surface, have weaker interfacial electronic coupling and as a result only participate once the electrochemical driving force is sufficient to overcome this weaker coupling (*22*). For our purposes, the slope depends on the ratio (υ/k_0) between the turnover rate of the enzyme (υ, the steady state velocity observed at a given substrate concentration) and the electrochemical electron exchange rate constant (k_0, the rate of electron exchange at zero driving force), noting that there is a dispersion in k_0 values due to enzyme molecules adopting slightly different orientations in the film.

The model predicts that the residual slope is proportional to the unattained limiting current and increases with any factor increasing the rate of turnover with respect to electron transfer; therefore, this slope can be used to extract catalytic parameters. As the turnover rate increases, limitations due to poor electron transfer become more visible (*22*). In accordance with this prediction, Figure 7B shows that the residual slope increases as the temperature is raised, as expected if the activation energy for enzyme turnover is higher than that for long-range electron transfer. In Figure 7A, the residual slope observed after baseline correction also increases with increasing substrate concentration, showing a hyperbolic dependence that was treated conventionally to obtain a K_M of 6 μM (the Hanes plot is shown in inset). This agrees very well with the value of 8 μM determined from solution assays under similar conditions (*11*).

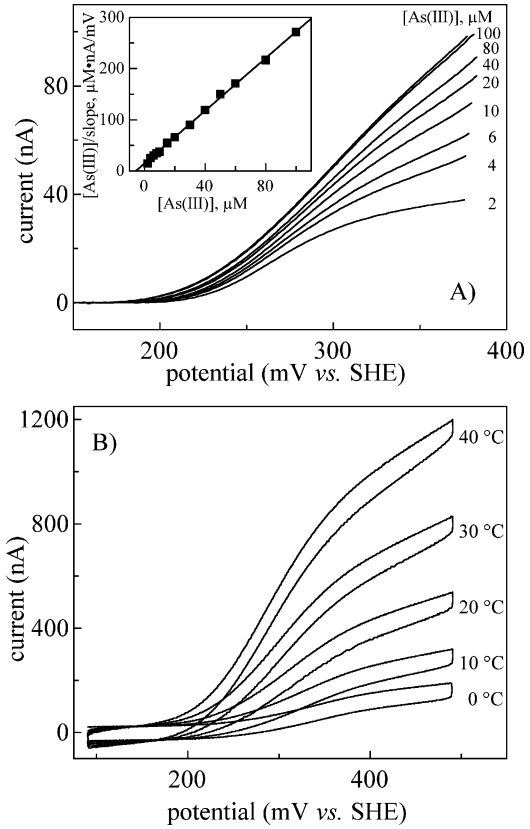

FIGURE 7: (A) Effect of increasing arsenite concentration on the oxidation current and residual slope at high potential. Conditions are as follows: 2−100 μM arsenite; pH 6.0; 25 °C; 20 mM MES; 100 mM NaCl; electrode rotation rate, 2400 rpm. Inset: A plot of the residual slope in a Hanes plot gives a K_M of 6 μM (*x*-intercept). (B) Effect of increasing temperature from 0 to 40 °C on activity with 100 μM arsenite for another film of arsenite oxidase. As evident from the amount of current generated, this film was remarkably electroactive. An increase in residual slope is observed with increasing temperature. Conditions are as follows: pH 6; 20 mM MES; 100 mM NaCl; electrode rotation rate, 2400 rpm.

In experiments with different electroactive coverages, K_M does not vary. However, variations in electroactive coverage and degree of electronic coupling with the electrode surface give differing catalytic currents, making it difficult to estimate a value for the turnover number, k_{cat}, especially when a limiting current plateau is not attained. Using the data from Figure 7B (where the arsenite concentration is much greater than K_M) and taking a value of at least 0.6 μA for the limiting current at 25 °C and a value of 2 pmol/cm^2 as an upper limit for the electroactive coverage (see above), we obtain a lower limit for the turnover number k_{cat} of about 50 s^{-1}.[3] For comparison, solution studies with azurin as the electron acceptor give a value of 27 s^{-1} under equivalent conditions (*11*). The electrochemical results are therefore consistent with the enzyme being fully active, although it is possible that higher activity might be attained than is measured conventionally since the electrode can provide whatever driving force is needed to optimize the catalytic rate (*12*).

DISCUSSION

Molybdenum Center. The only signal clearly discernible by cyclic voltammetry in the absence of substrate is a reversible couple centered at 292 mV vs. SHE at pH 5.9 and 0 °C, with a cooperativity coefficient, n_{app}, greater than one, attributable to the Mo(VI)/Mo(IV) redox couple. Both oxidation and reduction peaks are narrow, with an average width at half-height of 63 mV. Because the theoretical value for a one-electron signal is 83 mV at 0 °C and the width is inversely proportional to the number of electrons transferred cooperatively in the process, we conclude that the signal arises from the cooperative transfer of two electrons for both the oxidation and the reduction of the molybdenum center of arsenite oxidase. The reason that this signal is so prominent, and hence detectable, is that a highly cooperative two-electron center produces peaks that are up to four times higher and half as wide as those for a one-electron center (*13*−*15*). No EPR signals due to Mo(V) have been detected, supporting the conclusion that the Mo(VI/IV) couple is highly cooperative. If indeed the two-electron Mo(VI/IV) couple is fully cooperative, the signals should have a half-height width of just 42 mV. That the observed width is larger than the theoretical value most likely arises from environmental inhomogeneity among the adsorbed enzyme molecules (a situation that also has distinctive effects on the catalytic voltammetry—vide infra).

The reported crystal structure is of the reduced form of arsenite oxidase and shows the molybdenum coordination geometry to be five-coordinate, square pyramidal. From XAS studies of the enzyme (*24*), a Mo═O group is present in the reduced form but the identity of an additional O atom ligand in the oxidized form is ambiguous, being either oxo or hydroxo. Resonance Raman spectroscopy strongly suggests that this additional oxygen ligand, present in the oxidized enzyme, is an elongated oxo (*24*). The most likely explanation for the transfer of two protons upon electrochemical oxidation without the presence of a p*K* transition over the range of pH 5−10 is that they are derived from a noncoordinated water in the Mo(IV) state, leaving an unprotonated oxo in the Mo(VI) state:

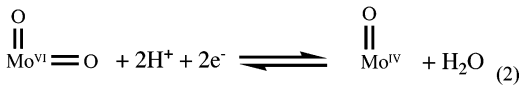

(2)

The present PFV results thus support the assignment of the active site in the oxidized state as an asymmetric dioxo center, L_2MoO_2, rather than (a protonated) $L_2MoO(OH)$.

The implication is that arsenite oxidase utilizes a "spectator oxo" effect (*25*) such as that described for sulfite oxidase and other $LMoO_2$(-S-cys)-containing enzymes (*26*, *27*). In this mechanism, the two Mo═O ligands effectively compete with one another in back-donating electron density into the molybdenum d-orbitals via π-interactions—the loss of one Mo═O upon reduction allows the remaining oxo group to bind more strongly, becoming a Mo≡O (triple) bond. This recovers some of the enthalpic cost of reaction and effectively labilizes the departing oxo group. The same mechanism in the L_2MoO_2 center of arsenite oxidase would make the molybdenum center a stronger oxo donor than would otherwise be the case, as is observed in model systems (*28*). A serine or cysteine ligand is present in other members of the DMSO reductase family and can act as a π-donor to the

[3] The turnover number is estimated from the limiting current, i_{lim}, at saturating substrate concentration using the relationship $k_{cat} = i_{lim}/n_sA\Gamma F$, where Γ represents the electroactive surface coverage for the enzyme on an electrode of surface area A (*23*).

metal center and thereby labilize the oxo group (*29*). Arsenite oxidase lacks such a ligand, but the spectator oxo effect can provide an alternative mechanism for efficient oxo transfer. Furthermore, the spectator oxo effect is also expected to reinforce the effect of geometric constraints placed on the molybdenum center by the polypeptide, in which a geometry more closely resembling that preferred by the reduced center is forced on the oxidized form, further labilizing the oxo group (*30*). This generation of an "entatic state" is thought to be common to all members of the DMSO reductase family of molybdenum enzymes. Together, these considerations account for the unusually high reduction potential for the molybdenum center of arsenite oxidase, i.e., a potential greater than that of arsenite [134 mV at pH 6 (*31*)], and ensure the thermodynamic favorability of arsenite oxidation by the enzyme.

Iron−Sulfur Clusters. The presence of two Fe−S clusters as auxiliary electron transport sites makes it easier for arsenite oxidase to undergo cooperative two-electron transfer by providing ready storage for electrons in the absence of a Mo(V) intermediate. This contrasts with sulfite oxidase from chicken liver, the most well-characterized example of a molybdoenzyme using a spectator oxo mechanism (*27*), for which there is only a single auxiliary cofactor (a b-type heme), and a Mo(V) intermediate is readily seen by EPR (*1*). To assess their role in electron transfer and storage, extensive efforts were made to identify signals due to the Fe−S clusters by cyclic voltammetry. However, on the basis of the fact that the two-electron signal assigned to Mo(VI)/Mo(IV) is already of low intensity, it is not surprising that any peaks from the one-electron Fe−S centers—typically one-fourth the height and twice the width of the two-electron peaks and probably broadened from their ideal shapes—are indistinguishable from the background current. Instead, we used spectrophotometric reductive titrations to obtain estimates for the reduction potentials of the Fe−S clusters.

The structure of arsenite oxidase indicates that the Rieske center has a nearby disulfide bridge holding the cluster-binding loop tightly together, typical of the higher potential Rieske centers found in the bc1-type enzymes (100−400 mV) as opposed to the Rieske type centers found in dioxygenases (typically −100 to −200 mV) (*32*, *33*). While the reduction potential determined here, ∼130 mV at pH 6 and 20 °C, is lower than that for most other "high potential" Rieske centers, it does fall within the range observed for this group. This wide range of potentials reported for such iron−sulfur clusters has been attributed to the variability in the number of hydrogen bonds in the core structure and the degree of solvent exposure (*34*, *35*).

The [3Fe−4S] cluster has a relatively high potential value, 260−270 mV at pH 6 and 20 °C. This is unusual, although a potential of 260 mV has been reported for a mutant [3Fe−4S] cluster created from a [4Fe−4S] cluster in a DMSO reductase (*36*). It is noteworthy that in this example, a serine is introduced at the "empty" corner of the cubane core, as is the case naturally for arsenite oxidase (*10*). In earlier work (*11*), it was seen that the EPR titration of the [3Fe−4S] cluster seemed to correlate very well with the optical changes at 682 nm typically associated with Mo absorption. From the results of the spectrophotometric titrations reported here, it is evident that the apparent correlation of the optical changes at 682 nm to the EPR signal of the [3Fe−4S] cluster is due simply to the similarity in potential of the Mo and [3Fe−4S] sites at the pH used in the measurements.

Catalytic Voltammetry. The catalytic voltammetry of arsenite oxidase yields kinetic parameters, k_{cat} and K_M, similar to the values observed in conventional solution studies, confirming that the adsorbed enzyme is fully active and functioning natively. The presence of a distribution of enzyme orientations having a varying degree of electronic coupling with the electrode surface, as evident from the appearance of residual slope in the catalytic voltammograms, suggests that the signals observed in nonturnover voltammetry must be broadened from their ideal values. This indicates that the degree of cooperativity seen in the nonturnover voltammetry is an underestimate and further supports the proposal that the molybdenum center of arsenite oxidase possesses a highly cooperative two-electron redox couple. This does not mean that concerted two-electron transfer takes place, which is highly unlikely given that the one-electron Fe−S clusters lie in a linear arrangement with the Mo center. However, it does mean that the extremely unstable semireduced forms of the enzyme with one electron on the molybdenum and the other on an Fe−S cluster will not accumulate and be detected during the time scale of a mixing experiment.

Concluding Remarks. In the present work, we have used PFV to probe a system whose electrochemical properties are difficult to address by other methods. The demonstration that the reversible oxidation and reduction of the molybdenum center is a cooperative, two-electron process accounts for the failure in earlier work to observe an EPR active Mo(V) state under a variety of conditions. Although unusual for a molybdenum enzyme of the L_2MoOX family, the result is fully consistent with the enzyme functioning as an oxo transferase (*37*, *38*), utilizing obligate two-electron chemistry to carry out the oxidation of substrate. The nature of the reaction has a precedent with the chemistry of Mo(VI)O_2/Mo(IV)O model systems (*26*−*28*, *30*, *37*, *38*), where a "spectator oxo" effect contributes significantly to decreasing the overall thermodynamic barrier to the reaction. In addition, as with related enzyme systems, the active site of oxidized arsenite oxidase is predisposed in an "entatic state" that also contributes to facile reduction and labilization of the oxo group. These two effects combine to maximize metal oxo labilization and is of great significance for arsenite oxidase, which lacks the protein-provided ligand typical of its family.

ACKNOWLEDGMENT

We thank Ms. Amy Stockert for preparation of xanthine oxidase and Dr. Christophe Léger for helpful discussions concerning analysis of the voltammetric data.

REFERENCES

1. Hille, R. (1996) *Chem. Rev. 96*, 2757−2816.
2. Bray, R. C., Adams, B., Smith, A. T., Richards, R. L., Lowe, D. J., and Bailey, S. (2001) *Biochemistry 40*, 9810−9820.
3. Bennett, B., Benson, N., McEwan, A. G., and Bray, R. C. (1994) *Eur. J. Biochem. 225*, 321−331.
4. Vincent, S. P., and Bray, R. C. (1978) *Biochem. J. 171*, 639−647.
5. Bray, R. C., and George, G. N. (1985) *Biochem. Soc. Trans. 13*, 560−567.
6. Vincent, S. P. (1979) *Biochem. J. 177*, 757−759.

7. Santini, J. M., Sly, L. I., Schnagl, R. D., and Macy, J. M. (2000) *Appl. Environ. Microbiol. 66*, 92−97.
8. Lebrun, E., Brugna, M., Baymann, F., Muller, D., Lièvremont, D., Lett, M.-C., and Nitschke, W. (2003) *Mol. Biol. Evol. 20*, 686−693.
9. Oremland, R. S., and Stolz, J. F. (2003) *Science 300*, 939−944.
10. Ellis, P. J., Conrads, T., Hille, R., and Kuhn, P. (2001) *Structure 9*, 125−132.
11. Anderson, G. L., Williams, J., and Hille, R. (1992) *J. Biol. Chem. 267*, 23674−23682.
12. Léger, C., Elliott, S. J., Hoke, K. R., Jeuken, L. J. C., Jones, A. K., and Armstrong, F. A. (2003) *Biochemistry 42*, 8653−8662.
13. Heering, H. A., Weiner, J. H., and Armstrong, F. A. (1997) *J. Am. Chem. Soc. 119*, 11628−11638.
14. Bard, A. J., and Faulkner, L. R. (2001) *Electrochemical Methods: Fundamentals and Applications*, 2nd ed., John Wiley & Sons, New York.
15. Plichon, V., and Laviron, E. (1976) *J. Electroanal. Chem. 71*, 143−156.
16. Jeuken, L. J. C., McEvoy, J. P., and Armstrong, F. A. (2002) *J. Phys. Chem. B 106*, 2304−2313.
17. Sucheta, A., Cammack, R., Weiner, J. H., and Armstrong, F. A. (1993) *Biochemistry 32*, 5455−5465.
18. Léger, C., Heffron, K., Pershad, H. R., Maklashina, E., Luna-Chavez, C., Cecchini, G., Ackrell, B. A. C., and Armstrong, F. A. (2001) *Biochemistry 40*, 11234−11245.
19. Massey, V. (1991) in *10th International Symposium of Flavins and Flavoproteins (1990)* (Curti, B., Ronchi, S., and Zanetti, G., Eds.) pp 59−66, de Gruyter, Berlin.
20. Kim, J. H., and Hille, R. (1993) *J. Biol. Chem. 268*, 44−51.
21. Szentrimay, R., Yeh, P., and Kuwana, T. (1977) in *Electrochemical Studies of Biological Systems* (Sawyer, D. T., Ed.) pp 143−169, The American Chemical Society, Washington, DC.
22. Léger, C., Jones, A. K., Albracht, S. P. J., and Armstrong, F. A. (2002) *J. Phys. Chem. B 106*, 13058−13063.
23. Heering, H. A., Hirst, J., and Armstrong, F. A. (1998) *J. Phys. Chem. B 102*, 6889−6902.
24. Conrads, T., Hemann, C., George, G. N., Pickering, I. J., Prince, R. C., and Hille, R. (2002) *J. Am. Chem. Soc. 124*, 11276−11277.
25. Rappé, A. K., and Goddard, W. A., III (1982) *J. Am. Chem. Soc. 104*, 3287−3294.
26. Peariso, K., McNaughton, R. L., and Kirk, M. L. (2002) *J. Am. Chem. Soc. 124*, 9006−9007.
27. Pietsch, M. A., and Hall, M. B. (1996) *Inorg. Chem. 35*, 1273−1278.
28. Arzoumanian, H., Corao, C., Heinz, K., Lopez, R., and Teruel, H. (1992) *J. Chem. Soc., Chem. Commun.*, 856−858.
29. Davie, S. R., Rubie, N. D., Hammes, B. S., Carrano, C. J., Kirk, M. L., and Basu, P. (2001) *Inorg. Chem. 40*, 2632−2633.
30. Thomson, L. M., and Hall, M. B. (2001) *J. Am. Chem. Soc. 123*, 3995−4002.
31. Pourbaix, M. (1966) *Atlas of Electrochemical Equilibria*, Pergamon Press, Oxford.
32. Zu, Y., Fee, J. A., and Hirst, J. (2002) *Biochemistry 41*, 14054−14065.
33. Link, T. A. (1999) in *Advances in Inorganic Chemistry: Iron−Sulfur Proteins* (Sykes, A. G., and Cammack, R., Eds.) pp 83−157, Academic Press, San Diego.
34. Hunsicker-Wang, L. M., Heine, A., Chen, Y., Luna, E. P., Todaro, T., Zhang, Y. M., Williams, P. A., McRee, D. E., Hirst, J., Stout, C. D., and Fee, J. A. (2003) *Biochemistry 42*, 7303−7317.
35. Colbert, C. L., Couture, M. M.-J., Eltis, L. D., and Bolin, J. T. (2000) *Structure 8*, 1267−1278.
36. Trieber, C. A., Rothery, R. A., and Weiner, J. H. (1996) *J. Biol. Chem. 271*, 4620−4626.
37. Schultz, B. E., Hille, R., and Holm, R. H. (1995) *J. Am. Chem. Soc. 117*, 827−828.
38. Caradonna, J. P., Reddy, P. R., and Holm, R. H. (1988) *J. Am. Chem. Soc. 110*, 2139−2144.

BI0357154